Desaturases: Emerging Models for Understanding Functional Diversification of Diiron-containing Enzymes*

John Shanklin[‡1], **Jodie E. Guy**[§], **Girish Mishra**[‡], **and Ylva Lindqvist**[§]

From the [‡]Department of Biology, Brookhaven National Laboratory, Upton, New York 11973 and the [§]Department of Medical Biochemistry and Biophysics, Karolinska Institutet, S-171 77 Stockholm, Sweden

Desaturases and related enzymes perform O_2-dependent dehydrogenations initiated at unactivated C-H groups with the use of a diiron active site. Determination of the long-sought oxidized desaturase crystal structure facilitated structural comparison of the active sites of disparate diiron enzymes. Experiments on the castor desaturase are discussed that provide experimental support for a hypothesized ancestral oxidase enzyme in the context of the evolution of the diiron enzyme diverse functionality. We also summarize recent analysis of a castor mutant desaturase that provides valuable insights into the relationship of proposed substrate-binding modes with respect to a range of catalytic outcomes.

Desaturase enzymes perform dehydrogenation reactions that result in the introduction of double bonds into fatty acids that are initiated by the energy-demanding abstraction of a hydrogen from a methylene group (1–3). To achieve this, desaturase enzymes recruit and activate molecular oxygen with the use of an active-site diiron cluster (4). The diiron center is common to a variety of proteins, including methane monooxygenase, ribonucleotide reductase, rubrerythrins, and a variety of oxidase enzymes (5). Valuable insights regarding the tuning of diiron centers with respect to diverse chemical reactivity (6) have been made via comparisons of the diiron centers of diiron-containing enzymes (7); however, differences in amino acid sequence, multiple protein-protein interactions, and reaction outcomes complicate the analysis. The study of fatty-acid desaturases and related enzymes presents a unique opportunity for performing enzyme structure-function studies because relatively close homologs perform diverse reactions on similar substrates (8, 9).

Desaturase enzymes have evolved independently twice (10); the acyl-ACP[2] desaturases are soluble enzymes found in the plastids of higher plants, whereas the more widespread class of integral membrane desaturases is found in endomembrane systems in prokaryotes and eukaryotes (9). In addition to forming distinct homology groups, their diiron centers possess distinct primary ligation spheres (11). The availability of crystal structures for acyl-ACP desaturases (12) makes this system amenable to detailed structure-function studies. Crystal structures are available for the 18:0 Δ^9-desaturase[3] (12, 13) from *Ricinus communis* (castor) and a bifunctional desaturase from *Hedera helix* (ivy) (14, 15). These desaturases are homodimeric proteins, with each monomer folded into a compact single domain composed of nine helices. The diiron active site of these enzymes is buried within a core four-helix bundle and is positioned alongside a deep, bent, narrow hydrophobic cavity in which the substrate is bound during catalysis. It is a textbook example of a lock-and-key type of binding site in which the bound fatty acid moiety is poised for formation of the *cis*-fatty acid product.

Nobel Laureate Konrad Bloch observed, "The stereospecific removal of hydrogen in the formation of oleate, although predictable on principle grounds would seem to approach the limits of the discriminatory power of enzymes" (16). Bloch's statement underscores that desaturase enzymes perform highly regio- and stereo-selective reactions on long-chain fatty acids composed of essentially equivalent methylene chains that lack distinguishing landmarks close to the site of desaturation. We will review structural features of the diiron active site of the acyl-ACP desaturases in the context of those of other diiron enzymes, discuss recent insights into the evolution of acyl-ACP desaturases, and summarize recent discoveries relating to the evolution of selectivity and functional diversity within desaturase enzyme families.

Organization of the Desaturase Diiron Site

The structure of the castor acyl-ACP desaturase shows the diiron active site in the reduced Fe(II)-Fe(II) form (13, 17). In the reduced active site (Fig. 1A), the two irons are separated by a distance of ~4.2 Å, and each is five-coordinate with a distorted square pyramidal geometry, giving a highly symmetrical structure to the diiron site. Fe1 is coordinated by Glu[105] in a bidentate manner and by a single interaction with His[146]. Both Glu[143] and Glu[229] bridge the two iron ions, with each residue forming one interaction with Fe1 and one with Fe2, whereas Glu[196] and His[232] are bidentate and monodentate ligands to Fe2, respectively. A water molecule is seen in the vicinity of the diiron site, but, with distances of 3.0 Å to Fe1 and 3.3 Å to Fe2, it is not in the first coordination shell of either iron ion.

The castor desaturase structure, together with extensive spectroscopic data (3), provided detailed knowledge of the Fe(II)-Fe(II) active state of the enzyme, but the structure of the Fe(III)-Fe(III) resting state remained elusive until studies of the ivy desaturase designed to reveal the basis for substrate

[3] In the fatty acid nomenclature used, *i.e. x:y*, *x* is the number of carbon atoms in the fatty acid chain, and *y* is the number of double bonds. Δ^x indicates the regiospecificity, *i.e.* the position of the double bond relative to the carboxyl-terminal end of the fatty acid.
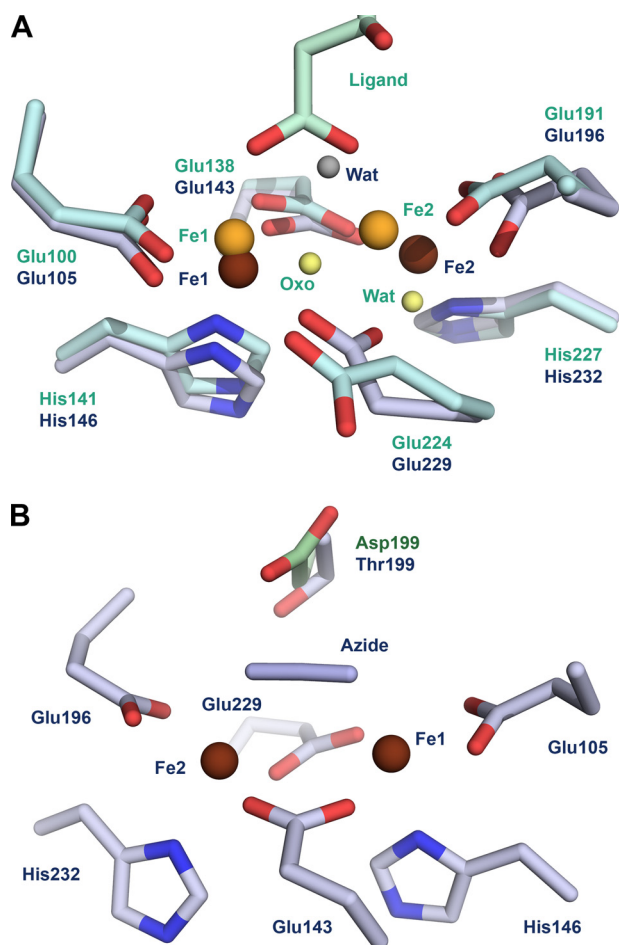
A

B

FIGURE 1. **Superimposition of the reduced active site of the castor desaturase and the oxidized active site of the ivy desaturase.** *A,* the reduced active site is shown in *blue gray,* with *brown* irons and *gray* water (*Wat*). The oxidized active site is shown in *cyan,* with *orange* iron ions, and the μ-oxo bridge and water are depicted in *yellow*. *B,* the active-site residues of the azide complex of the castor desaturase are shown, with colors the same as those described for *A* and with Thr[199] included. The Asp[199] side chain of the T199D mutant is superimposed on the structure and is depicted in *green*. Note that the view is from the opposite face of the active site with respect to *A* to clearly show the position of the mutation.

specificity unexpectedly provided the first structure of the oxidized active site (15). In this structure (Fig. 1*A*), the distance between the two irons is shorter, at ~3.2 Å, and a μ-oxo bridge links them. The decreased iron-iron distance results from a 1.3-Å shift in the position of Fe2, along with alterations to the coordination sphere of the diiron site. The bidentate glutamic acids coordinating each iron (Glu[100] and Glu[191]) remain, as do the histidine coordinating Fe1 (His[141]) and one of the bridging glutamic acids (Glu[138], which is equivalent to Glu[143] of the castor structure). However, Glu[224] (Glu[229] in castor), which is the second bridging carboxylate in the reduced structure, undergoes a large carboxylate shift in the oxidized structure to leave the side chain pointing away from the diiron center, *i.e.* making no interaction with either iron. The Glu[224] carboxylate shift creates space for the μ-oxo bridge, which is positioned on the same side of the diiron site. His[227] (castor His[232]) is replaced by a water molecule, and it therefore interacts with Fe2 only weakly via the water molecule. In the ivy desaturase structure, the remaining coordination position of each iron is occupied by

a bidentate small molecule ligand, which appears to be a 3-hydroxy fatty acid thought to have originated from the expression host *Escherichia coli*. Further work will establish which, if any, of the changes seen for the oxidized structure are influenced by the presence of the ligand.

In contrast to the soluble desaturases, evidence for a diiron active site in the integral membrane desaturases is indirect, based on the presence of a conserved and catalytically essential tripartite 8-histidine motif (11) within domains corresponding to equivalents found in the spectroscopically characterized alkane ω-hydroxylase from *Pseudomonas oleovorans* (50, 51).

Comparison of the Desaturase Active Site with Those of Other Diiron Proteins

Although several excellent reviews (*e.g.* Ref. 7) have provided valuable insights into differences in diiron protein function, these studies were hampered by the lack of an oxidized desaturase structure. The oxidized desaturase active site shares several key features with the corresponding structure of MMO (18), in contrast to the reduced structures of the desaturase and its azide complex, which bear striking similarities to those of rubrerythrin oxidase (13, 19). In the desaturase and MMO, μ-oxo bridges are formed on the same side of the diiron axis, whereas the μ-oxo bridge of the oxidized rubrerythrin active site is situated on the opposite side, in the same position to which azide can bind in the reduced structure (19). As described above, upon oxidation of the desaturase active site, Glu[224] changes from being a bridging ligand in the reduced form to making no direct interaction with either iron in the oxidized form. In other proteins in which a carboxylate shift is observed, the affected side chain retains coordination with one iron. In addition, the lack of histidine coordination to Fe2 in the oxidized structure is also unique to the desaturase. In rubrerythrin, the histidine coordinating Fe2 is unchanged, whereas that coordinating Fe1 is lost, and in both MMO and ribonucleotide reductase R2, the coordination of both histidines remains constant in the oxidized and reduced states.

Evolution of Diiron Enzyme Functionality

Gomes *et al.* (20) rationalized that a progenitor diiron enzyme was likely an oxidase that would have arisen after the emergence of oxygen in the atmosphere to mitigate the deleterious effects of reactive oxygen species by reducing them to water. Support for this hypothesis came from structure-function experiments involving desaturase and a peroxidase, rubrerythrin (21). Despite poor overall homology between the enzymes, comparison of their active sites revealed a one-to-one correspondence between amino acid side chains comprising the diiron ligation sphere and remarkably similar geometry in their respective azide complexes (Fig. 1*B*). In both active sites, two glutamic acid side chains bridge the two Fe(II) ions, whereas each iron is also terminally coordinated by another glutamic acid and a histidine. The binding site of azide in the two active sites is almost identical and, in each case, occurs with little change to the coordination sphere and, in contrast to the azide complex of MMO, without a carboxylate shift.

Despite this similarity, a significant difference is seen between the two active sites; the desaturase contains a con-

served threonine in place of an aspartic acid, which, in the rubrerythrin, is immediately adjacent to the location of the activated oxygen species (21). The carboxylate in the rubrerythrin facilitates proton transfer to the activated oxygen, favoring oxidase chemistry, whereas the desaturase possesses a threonine, a poor proton donor, favoring hydrogen abstraction from the fatty acid substrate. The active site of the desaturase is also more isolated from solvent protons than that of rubrerythrin (22). Replacement of the conserved threonine for an aspartic acid resulted in an increase in the oxidase/desaturase ratio of 1.4×10^4 compared with the wild-type desaturase, providing experimental support for a relationship between desaturase and a hypothesized peroxidase ancestor. Co-opting a peroxidase enzyme architecture to utilize a bound activated oxygen for reactions such as fatty acid desaturation would involve gaining the ability 1) to bind unactivated oxygen, 2) to interact with an electron transport chain to effect a 2-electron reduction, and 3) to bind substrate. In such a scenario, one might expect to identify primitive biosynthetic enzymes that use peroxide as the exclusive source of the activated oxygen used for catalysis. Although such enzymes have not been reported, others such as MMO and alkene monooxygenases that obtain reducing equivalents from electron transport chains are also able to use the "peroxide shunt" (23), which may represent an artifact of such an evolutionary ancestry.

Evolution of Functionality within Desaturase Families

Soluble and integral membrane desaturases, *e.g.* from castor (10) and yeast (24), respectively, exclusively introduce double bonds into the Δ^9-position of saturated 16- and 18-carbon substrates. The close relationship of variant desaturase-like enzymes with their parental archetypes suggests that bifunctional enzymes retaining residual parental activity might exist. An interesting consequence of the existence of bi- or multifunctional enzymes is that they present the host organism with a range of potential biosynthetic outcomes based on expression of the enzymes in distinct tissues with different available substrates (25). An example of a bifunctional desaturase comes from the *Ceratodon* fatty-acyl acetylenase/desaturase, which performs two sequential dehydrogenation reactions at the Δ^6-position, the first introducing a double bond and the second a triple bond. How acetylenases abstract two hydrogens from adjacent carbon atoms linked by a double bond without forming an epoxide remains an intriguing mechanistic question. There are several examples of bifunctional desaturases, including the tung conjugase/desaturase, which converts 18:$2\Delta^{9-cis,12-cis}$ to 18:$3\Delta^{9-cis,11-trans,13-trans}$ and also converts 18:$1\Delta^{9-cis}$ to 18:$2\Delta^{9-cis,12-trans}$ (25). The *Lesquerella* hydroxylase/desaturase involves the introduction of distinct functionality, either a double bond or a hydroxy group at C-12 (26). It is an example of a desaturase enzyme with intermediate functionality between that of the oleate Δ^{12}-desaturase and the castor 12-hydroxylase. A mechanistic link between hydroxylase enzymes and desaturases was supported by close examination of the products of desaturases from a range of sources that revealed trace amounts of hydroxylation activity (27). Indeed, for cases in which the cryptoregiochemistry (1) has been determined, there is a correspondence between trace levels of hydroxylation at a particular carbon and the site of initial oxygen attack (27).

Regioselectivity in acyl-ACP desaturases has been hypothesized to evolve by changes in as few as four specific amino acid locations (15, 28). For membrane desaturases, substrate factors have also been shown to influence regioselectivity. For instance, the regioselectivity of a bifunctional 16:0 Δ^7/Δ^9-desaturase was reported to be controlled by its subcellular targeting to different organelles in which the same fatty acid is esterified to different headgroups (29). In this case, the nature of the substrate headgroup, and not differences in the amino acid sequence of the enzymes or the fatty acid, determines regioselectivity.

Unusual Fatty Acid Biosynthesis by Desaturases and Related Enzymes

In addition to commonly occurring fatty acids 16 or 18 carbons in length and with between zero and three *cis* double bonds, upwards of 1,000 so-called unusual fatty acids have been identified (30) that, in addition to *cis* double bonds, contain various functional groups such as *trans* double bonds, hydroxy groups, epoxide groups, triple bonds, etc. (31). The enzymes responsible for the biosynthesis of unusual fatty acids recognize similar (or identical) substrates and, like desaturases, initiate catalysis by abstraction of a hydrogen from an unactivated methylene group (32), so it is not surprising that many of these enzymes evolved from desaturases. For example, the gene for the oleate 12-hydroxylase was cloned based on its predicted homology to the oleate Δ^{12}-desaturase (33). Substitution of five amino acids located adjacent to a cluster of active-site histidine residues (11) with their equivalents from the hydroxylase was sufficient to convert the desaturase into a hydroxylase (and vice versa) (34). Two of the five locations were shown to predominantly influence functional outcome (27). Lack of a membrane desaturase crystal structure precluded mechanistic interpretation of these intriguing results.

Acyl-ACP desaturases convert saturated fatty acyl-ACPs to their monounsaturated counterparts (9). They vary in both chain length selectivity and regioselectivity (35, 36). A comparison of the structures of the castor 18:0 Δ^9- and ivy 16:0 Δ^4-desaturases (14) was initiated to determine the basis for regioselectivity (15). A triple mutant designed to investigate the basis for regioselectivity retained its Δ^9-desaturation activity, converting 18:0 into 18:$1\Delta^{9-cis}$; however, this product was further metabolized to 9-OH 18:$1\Delta^{10-trans}$ (37) in a reaction reminiscent of the synthesis of dimorphecolic acid (9-OH 18:$2\Delta^{10-trans,12-trans}$) (38). Production of a *trans*-allylic alcohol by close relatives of both membrane and soluble classes of desaturases underscores the commonality of catalytic repertoire between these two classes of enzymes. When the 18:$1\Delta^{9-trans}$ substrate was presented to the enzyme, two products were synthesized: the 9-OH 18:1 Δ^{10-cis}-allylic alcohol and the $\Delta^{9-trans,11-cis}$-isomer of CLA. It was rationalized that the formation of the three unusual fatty acids in terms of distinct proposed substrate binding relative to the position of the oxidant and the bend in the active-site cavity (Fig. 2). Formation of the allylic alcohol results from the ability of the mutant to recognize its initial desaturation product, 18:$1\Delta^{9-cis}$, as a substrate (possibly because of alterations in
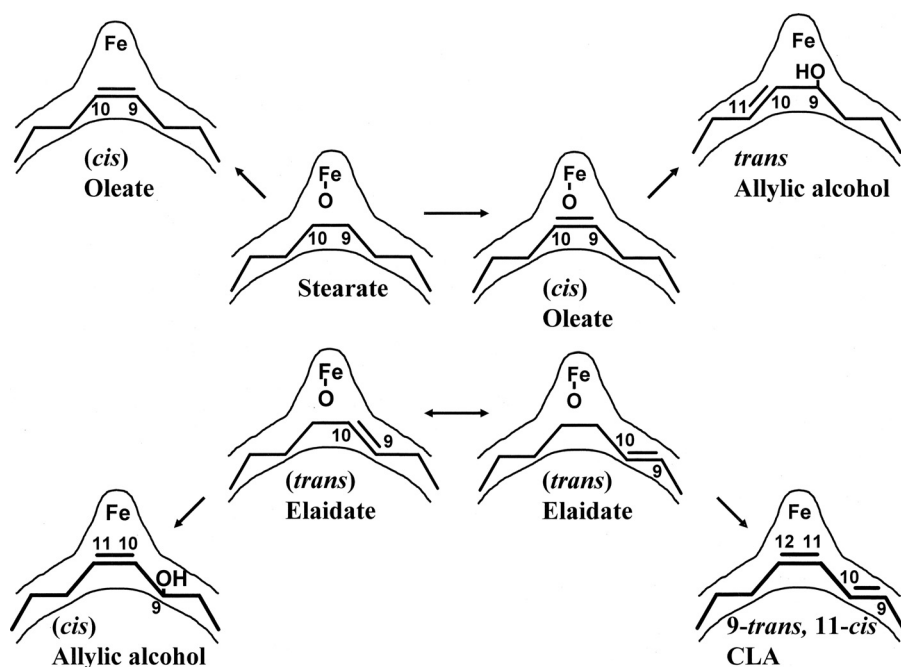
FIGURE 2. **Schematic representation of the proposed binding modes of substrate (inner) and their respective products (outer).** Note the substrate enters the channel from the right-hand side in the extended conformation.

binding affinity for $18:1\Delta^{9\text{-}cis}$ and/or changes in redox gating properties) (39). The C-10 double bond forms in the *trans* configuration because this region of the substrate is predicted to be in the anti-conformation. Lack of rotation around C-9 and C-10 of the $18:1\Delta^{9\text{-}trans}$ substrate would cause it to penetrate one carbon less deeply into the binding cavity and the *cis*-allylic alcohol would result from placement of C-10 and C-11 at the bend in the binding cavity, which would impose an eclipsed conformation. CLA formation would result from the $18:1\Delta^{9\text{-}trans}$ substrate binding two carbons less deeply in the active site, followed by a "normal" desaturation reaction in a fashion similar to that described for the conversion of the $18:1\Delta^{11\text{-}trans}$ substrate to CLA $\Delta^{9\text{-}cis,11\text{-}trans}$ by the wild-type desaturase (40).

Register and Chemical Nature of the Substrate Affect Reaction Outcome

Residues attributed to binding the diiron site in both soluble and membrane desaturases are found in the same relative positions in the sequences of enzymes that exhibit diverse specificity and functional outcome. This implies the iron-bound oxidant occurs in fixed positions; thus, differences in catalytic activity are likely the result of differences in presentation of the substrate to the oxidant. This could occur via changes in the amino acid sequence of the enzyme close to the active site as was described for the oleate hydroxylase (27, 34) or from differences in the nature of the substrate that could perhaps subtly alter the register of the fatty acid in the binding cavity (37). Support for changes in register influencing reaction outcome comes from analysis of mutants of the oleate desaturase capable of hydroxylation, in which the hydroxylation/desaturation ratio was 5–9-fold higher for 18-carbon *versus* 16-carbon substrates (27). The presence of functional groups in the acyl chain can be

envisaged to affect the substrate-binding mode as described above for the variant soluble desaturase (37).

The principle that existing modifications can lead to further changes in substrate binding relative to the active-site oxidant offers an appealing explanation for the observation that many unusual fatty acids contain multiple unusual functionalities within the same acyl chain (31, 41). For instance, the occurrence of triple bonds in acyl chains is often associated with the introduction of additional acetylenic groups or ω-hydroxylation (31). The presence of a triple bond in a substrate imparts rotational and rigidity constraints in addition to a reduced C–C bond length to a portion of the acyl chain that restricts its potential binding modes relative to a substrate lacking the acetylenic group. An interesting example of this was recently reported for a desaturase from *Thaumetopoea* that is responsible for the production of an unusual fatty acid sex pheromone, 11-ynoic $16:1\Delta^{13}$, which is produced from 16:0 (42). The enzyme initially desaturates 16:0 at the Δ^{11}-position and then performs a second C-11 desaturation to introduce the triple bond. The acetylenic substrate, containing a linear rigid portion at C-11–C-12, is unable to bind in the presumed bend in the substrate-binding cavity, and so *cis* dehydrogenation occurs at the next rotationally flexible carbons, *i.e.* C-13 and C-14, yielding the 11-ynoic $\Delta^{13\text{-}cis}$-product. Another example of sequential functionality has been reported in fungi, which have a desaturase that introduces two double bonds via sequential desaturation, the first at Δ^{12} and the second at the ω-3 position (43), presumably because of changes in binding mode due to the introduction of the *cis* Δ^{12}-double bond. These examples of individual enzymes catalyzing sequential reactions support the notion that modifications to the physical nature of the substrate can result in discrete binding modes that favor distinct reactions within the same enzyme. Interestingly, whereas *trans* double or acetylenic bonds in the substrate often correlate with unusual fatty acid production, the presence of hydroxy groups has been shown to be functionally equivalent to *cis* double bonds with respect to the placement of subsequent double bonds (44).

Enzyme-Substrate Interactions for Soluble and Membrane Desaturases

There are many similarities between the chemistry performed by soluble and membrane-bound desaturases. Both perform regioselective *cis* dehydrogenation, a process that requires tight binding of the substrate in the eclipsed conformation. That both perform pro-*R* dehydrogenation implies that the oxidant lies on the same side of the substrate-binding plane

for both classes of enzymes. There are also notable differences. For instance, it was shown that replacing the pendant alkyl group of methyl 9-thiastearate with a benzyl moiety had no effect on the enantioselectivity of sulfoxidation by yeast, implying that the bulky benzyl group did not impede substrate access to the active site (45). Also, sterculic (8-(2-octacyclopropen-1-yl)octanoic) acid with its bulky cyclopropene ring is a potent inhibitor of membrane stearoyl-CoA desaturases but not of acyl-ACP desaturases (46–48) presumably because it is too bulky to enter the narrow substrate-binding channel of the soluble desaturases (17). This suggests that the membrane desaturase active site has a fundamentally different architecture from that of the soluble desaturase, perhaps having a cleft into which substrates enter laterally rather than a deep binding cavity into which substrates enter in extended conformation as for the soluble desaturases. The two classes of desaturases also exhibit different rate-limiting steps. For the membrane desaturases, the initial C–H bond-breaking step is rate-limiting as evidenced by a large kinetic isotope effect upon substitution of deuterium for hydrogen, whereas little effect is seen for the soluble desaturase (1). The limiting step for the soluble desaturase may be the release of acyl-ACP product, which involves the energetically unfavorable solvation of hydrophobic product as it leaves the hydrophobic cavity and enters the aqueous phase. This is in contrast to the membrane desaturases, in which the lipid-linked product is released into the lipid comprising the membrane.

The determination of a crystal structure of a member of the membrane class of desaturases would transformationally improve our understanding of the structure-function relationships of this functionally diverse family of proteins. To achieve this, two major issues need to be resolved. First, a system for expression of functional desaturase needs to be established; and second, a method of purification with yields of active protein sufficient for structural analysis needs to be developed. An exciting advance in this direction is the report of the expression and purification of active human stearoyl-CoA desaturase (49).

REFERENCES

1. Buist, P. H. (2004) *Nat. Prod. Rep.* **21,** 249–262
2. Broadwater, J. A., and Fox, B. G. (1998) *Fett. Lipid* **100,** 103–113
3. Fox, B. G., Lyle, K. S., and Rogge, C. E. (2004) *Acc. Chem. Res.* **37,** 421–429
4. Fox, B. G., Shanklin, J., Somerville, C., and Münck, E. (1993) *Proc. Natl. Acad. Sci. U. S. A.* **90,** 2486–2490
5. Wallar, B. J., and Lipscomb, J. D. (1996) *Chem. Rev.* **96,** 2625–2658
6. Yoon, S., and Lippard, S. J. (2004) *J. Am. Chem. Soc.* **126,** 16692–16693
7. Sazinsky, M. H., and Lippard, S. J. (2006) *Acc. Chem. Res.* **39,** 558–566
8. Lee, M., Lenman, M., Banaś, A., Bafor, M., Singh, S., Schweizer, M., Nilsson, R., Liljenberg, C., Dahlqvist, A., Gummeson, P. O., Sjödahl, S., Green, A., and Stymne, S. (1998) *Science* **280,** 915–918
9. Shanklin, J., and Cahoon, E. B. (1998) *Annu. Rev. Plant Physiol. Plant Mol. Biol.* **49,** 611–641
10. Shanklin, J., and Somerville, C. (1991) *Proc. Natl. Acad. Sci. U. S. A.* **88,** 2510–2514
11. Shanklin, J., Whittle, E., and Fox, B. G. (1994) *Biochemistry* **33,** 12787–12794
12. Lindqvist, Y. (2001) *Δ⁹-Stearoyl-acyl Carrier Protein Desaturase*, John Wiley & Sons, Chichester, United Kingdom
13. Moche, M., Shanklin, J., Ghoshal, A., and Lindqvist, Y. (2003) *J. Biol. Chem.* **278,** 25072–25080
14. Whittle, E., Cahoon, E. B., Subrahmanyam, S., and Shanklin, J. (2005) *J. Biol. Chem.* **280,** 28169–28176
15. Guy, J. E., Whittle, E., Kumaran, D., Lindqvist, Y., and Shanklin, J. (2007) *J. Biol. Chem.* **282,** 19863–19871
16. Bloch, K. (1969) *Acc. Chem. Res.* **2,** 193–202
17. Lindqvist, Y., Huang, W., Schneider, G., and Shanklin, J. (1996) *EMBO J.* **15,** 4081–4092
18. Rosenzweig, A. C., Frederick, C. A., Lippard, S. J., and Nordlund, P. (1993) *Nature* **366,** 537–543
19. Jin, S., Kurtz, D. M., Jr., Liu, Z. J., Rose, J., and Wang, B. C. (2002) *J. Am. Chem. Soc.* **124,** 9845–9855
20. Gomes, C. M., Le Gall, J., Xavier, A. V., and Teixeira, M. (2001) *ChemBioChem.* **2,** 583–587
21. Guy, J. E., Abreu, I. A., Moche, M., Lindqvist, Y., Whittle, E., and Shanklin, J. (2006) *Proc. Natl. Acad. Sci. U. S. A.* **103,** 17220–17224
22. Shanklin, J., and Whittle, E. (2007) *Acyl-ACP Desaturase Architecture Favors High-energy Desaturation Reaction over Lower-energy Oxidase Chemistry*, Aardvark Global Publishing Co., LLC, Salt Lake City, UT
23. Fosdike, W. L., Smith, T. J., and Dalton, H. (2005) *FEBS J.* **272,** 2661–2669
24. Stukey, J. E., McDonough, V. M., and Martin, C. E. (1990) *J. Biol. Chem.* **265,** 20144–20149
25. Dyer, J. M., Chapital, D. C., Kuan, J. C., Mullen, R. T., Turner, C., McKeon, T. A., and Pepperman, A. B. (2002) *Plant Physiol.* **130,** 2027–2038
26. Broun, P., Boddupalli, S., and Somerville, C. (1998) *Plant J.* **13,** 201–210
27. Broadwater, J. A., Whittle, E., and Shanklin, J. (2002) *J. Biol. Chem.* **277,** 15613–15620
28. Cahoon, E. B., Lindqvist, Y., Schneider, G., and Shanklin, J. (1997) *Proc. Natl. Acad. Sci. U. S. A.* **94,** 4872–4877
29. Heilmann, I., Mekhedov, S., King, B., Browse, J., and Shanklin, J. (2004) *Plant Physiol.* **136,** 4237–4245
30. Millar, A. A., Smith, M. A., and Kunst, L. (2000) *Trends Plant Sci.* **5,** 95–101
31. Badami, R. C., and Patil, K. B. (1980) *Prog. Lipid Res.* **19,** 119–153
32. Buist, P. H. (2007) *Nat. Prod. Rep.* **24,** 1110–1127
33. van de Loo, F. J., Broun, P., Turner, S., and Somerville, C. (1995) *Proc. Natl. Acad. Sci. U. S. A.* **92,** 6743–6747
34. Broun, P., Shanklin, J., Whittle, E., and Somerville, C. (1998) *Science* **282,** 1315–1317
35. Haas, J. A., and Fox, B. G. (1999) *Biochemistry* **38,** 12833–12840
36. Whittle, E., and Shanklin, J. (2001) *J. Biol. Chem.* **276,** 21500–21505
37. Whittle, E. J., Tremblay, A. E., Buist, P. H., and Shanklin, J. (2008) *Proc. Natl. Acad. Sci. U. S. A.* **105,** 14738–14743
38. Cahoon, E. B., and Kinney, A. J. (2004) *J. Biol. Chem.* **279,** 12495–12502
39. Reipa, V., Shanklin, J., and Vilker, V. (2004) *Chem. Comm.* **21,** 2406–2407
40. Broadwater, J. A., Laundre, B. J., and Fox, B. G. (2000) *J. Inorg. Biochem.* **78,** 7–14
41. van de Loo, F. J., Fox, B. G., and Somerville, C. (1993) in *Lipid Metabolism in Plants* (Moore, T. S., ed) pp. 91–126, CRC Press, Boca Raton, FL
42. Serra, M., Piña, B., Abad, J. L., Camps, F., and Fabriàs, G. (2007) *Proc. Natl. Acad. Sci. U. S. A.* **104,** 16444–16449
43. Damude, H. G., Zhang, H., Farrall, L., Ripp, K. G., Tomb, J. F., Hollerbach, D., and Yadav, N. S. (2006) *Proc. Natl. Acad. Sci. U. S. A.* **103,** 9446–9451
44. Engeseth, N., and Stymne, S. (1996) *Planta* **198,** 238–245
45. Buist, P. H., and Marecak, D. M. (1992) *J. Am. Chem. Soc.* **114,** 5073–5080
46. Johnson, A. R., Pearson, J. A., Shenstone, F. S., and Fogerty, A. C. (1967) *Nature* **214,** 1244–1245
47. Soulard, P., McLaughlin, M., Stevens, J., Connolly, B., Coli, R., Wang, L., Moore, J., Kuo, M. S., LaMarr, W. A., Ozbal, C. C., and Bhat, B. G. (2008) *Anal. Chim. Acta* **627,** 105–111
48. Gomez, F. E., Bauman, D. E., Ntambi, J. M., and Fox, B. G. (2003) *Biochem. Biophys. Res. Commun.* **300,** 316–326
49. Goren, M. A., and Fox, B. G. (2008) *Protein Expression Purif.* **62,** 171–178
50. Shanklin, J., Achim, C., Schmidt, H., Fox, B. G., and Munck, E. (1997) *Proc. Natl. Acad. Sci. U. S. A.* **94,** 2981–2986
51. Shanklin, J., and Whittle, E. (2003) *FEBS Lett.* **545,** 188–192